ChemComm

Accepted Manuscript

This article can be cited before page numbers have been issued, to do this please use: Z. Yang, H. Zhang, B. Yu, Y. Zhao, Z. Ma, G. Ji, B. Han and Z. Liu, *Chem. Commun.*, 2015, DOI: 10.1039/C5CC03151F.

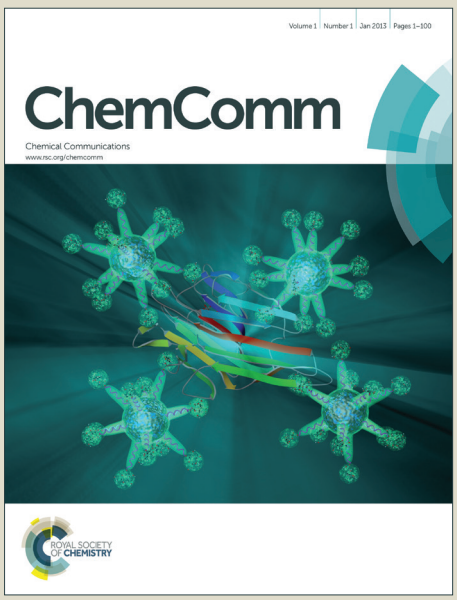

This is an *Accepted Manuscript*, which has been through the Royal Society of Chemistry peer review process and has been accepted for publication.

Accepted Manuscripts are published online shortly after acceptance, before technical editing, formatting and proof reading. Using this free service, authors can make their results available to the community, in citable form, before we publish the edited article. We will replace this *Accepted Manuscript* with the edited and formatted *Advance Article* as soon as it is available.

You can find more information about *Accepted Manuscripts* in the Information for Authors.

Please note that technical editing may introduce minor changes to the text and/or graphics, which may alter content. The journal's standard Terms & Conditions and the Ethical guidelines still apply. In no event shall the Royal Society of Chemistry be held responsible for any errors or omissions in this *Accepted Manuscript* or any consequences arising from the use of any information it contains.

ROYAL SOCIETY OF CHEMISTRY

www.rsc.org/chemcomm

View Article Online
DOI: 10.1039/C5CC03151F

ChemComm RSCPublishing

COMMUNICATION

Cite this: DOI: 10.1039/x0xx00000x

Azo-functionalized microporous organic polymers: Synthesis and applications in CO_2 capture and conversion

Received 00th January 2012,
Accepted 00th January 2012

DOI: 10.1039/x0xx00000x

www.rsc.org/

Zhenzhen Yang, Hongye Zhang, Bo Yu, Yanfei Zhao, Zhishuang Ma, Guipeng Ji, Buxing Han and Zhimin Liu*

Azo-functionalized MOPs (Azo-MOPs) was synthesized via oxidative polymerization of aromatic amines catalyzed by t-BuOCl/NaI (25 °C, 1 h, yield: >95%), which displayed excellent coordinating ability with Ru complex. The resultant Ru-coordinated Azo-MOPs displayed high CO_2 capacity and high performances for catalyzing the methylation of amines with CO_2 under low pressure (0.5 MPa).

The combination of CO_2 capture and conversion is an attractive strategy for efficiently reducing CO_2 emissions, simultaneously activating and transforming CO_2 into value-added chemicals. In this respect, microporous organic polymers (MOPs, pore diameters <2 nm), especially those embedded with CO_2-philic group may satisfy the requirements for the simultaneous capture and conversion of CO_2. As an emerging material platform, MOPs have attracted considerable scientific interest due to their distinctive properties such as large surface areas, low skeleton density, good physicochemical stability, wide-ranging flexibility in the choice and design of components and the available control of pore parameters.[1] MOPs have promising applications in the fields of gas adsorption (e.g. CO_2, H_2, CH_4), heterogeneous catalysis, electric energy storage and so on.[1-2] In particular, MOPs with nitrogen-rich functionalities, such as triazine,[3] tetrazole,[4] imidazole[5] and amines,[6] showed "CO_2-philic" property and superior capacity to CO_2 uptake, which is generally believed to arise from enhanced CO_2-framework interactions through hydrogen bonding and/or dipole-quadrupole interactions.[1] Due to their 3D open frameworks, MOPs constitute a new type of nanoreactor that allows the complementary utilization of skeletons and pores for integrating various functionalities (e.g. coordination with transition-metal complexes).[1-2, 7] Incorporation of metal-organic moieties in MOPs may lead to materials capable of both CO_2 capture and its simultaneous conversion. For example, Deng's group developed a class of Co/Al-coordinated conjugated microporous polymers that exhibit outstanding performance for CO_2 capture and further conversion via the reaction with epoxides at atmospheric pressure and room temperature.[8] The Tröger's base-derived MOPs coordinated with Ru showed good CO_2 and H_2 adsorbing performances, as well as high efficiency for catalyzing hydrogenation of CO_2 to HCOOH.[9]

Azo-bridged porous MOPs (Azo-MOPs) exhibited high CO_2 adsorption capacity (up to 236 mg g^{-1} at 273 K),[10] and the CO_2-philic nature may result in activation of CO_2. Being highly selective and sensitive toward the incorporation of various metal ions, the azo-type ligand is one of the most versatile ligands studied in coordination chemistry.[11] Hence, Azo-MOPs have the potential to act as heterogeneous supports for noble metal catalysts. The synthesis of the Azo-MOPs have been reported through direct coupling of aromatic nitro and amino compounds;[10a, 10d] however, it required high temperature (150 °C), and the product yields were relatively low (40-57%). Recently, the synthesis of porous azo-linked polymers was achieved by homocoupling of aniline-like building units in the presence of CuBr/pyridine (up to 80 °C, 48 h),[10b] or homocoupling of aromatic nitro monomers catalyzed by Zn/NaOH (65 °C, 36 h).[10c] Though such progress has been made, it is still desirable to develop simple and efficient route for the production of Azo-MOPs under mild and easy-handling conditions, especially at room temperature. Moreover, the specifically designed Azo-MOPs may be commendable candidates as adsorbents with high capacity of CO_2 and heterogeneous catalysts for efficient activation and transformation of CO_2 into value-added chemicals.

Inspired by the above progress and ideas, herein, we present a novel, simple and efficient method for the synthesis of Azo-MOPs through oxidative polymerization of aromatic multi-amines catalyzed by *t*-BuOCl/NaI, which could be performed rapidly at room temperature (e.g., 25 °C, 1 h), affording excellent product yields (>95%). The resultant Azo-MOPs

Beijing National Laboratory for Molecular Sciences, Key Laboratory of Colloid, Interface and Thermodynamics, Institute of Chemistry, Chinese Academy of Sciences, Beijing 100190, China
E-mail: liuzm@iccas.ac.cn
Electronic Supplementary Information (ESI) available: For experimental details and spectral data, See DOI: 10.1039/b000000x/

View Article Online
DOI: 10.1039/C5CC03153F
Journal Name

displayed high thermal stability up to 400°C, high Brunauer-Emmett-Teller (BET) surface areas up to 706 m^2 g^{-1} and high adsorption capacity to CO_2 of 134.8 mg g^{-1} (273 K). Furthermore, the Azo-MOPs could coordinate with Ru(III) complex, and the obtained materials (**Azo-MOP-Ru**) could serve as efficient adsorbents for CO_2 (up to 92.1 mg g^{-1} at 273 K) and displayed high performances and stability for catalyzing the methylation of amines with CO_2 under low pressure (0.5 MPa), together with broad scope of the reactants, excellent product yields (92%-99%), high stability and easy recyclability. The combination of two components (CO_2-philic azo groups and Ru-complex) led to functionalized MOPs that satisfy the requirements for effective CO_2 capture and conversion.

Four aromatic multi-amines with different geometry configurations including tetrakis(4-aminophenyl)methane (**A-1**), 2,6,14-triaminotriptycene (**A-2**), 1,3,5-tris(4-aminophenyl)benzene (**A-3**) and tris(4-aminophenyl)amine (**A-4**) were selected as the building blocks for the synthesis of Azo-MOPs via oxidative polymerization using *t*-BuOCl/NaI as the oxidant, as illustrated in Scheme 1. Notably, the polymerization of **A-N (N=1~4)** could occur very rapidly at room temperature (25°C, 1 h), and the product yield could reach >95%, much higher than those reported in literature.[10a, 10b] This means that the route developed for the synthesis of Azo-MOPs in this work was highly efficient. It was indicated that the yield, BET surface area (Figure S1, ESI) and morphology (Figure S2, ESI) of the polymer derived from **A-1** (denoted as **Azo-MOP-1**) was greatly affected by the solvents used in the synthetic process, which probably resulted from the different solvent power of the solvents for the polymer and also from the interactions between the monomers, oligomers, polymers and the reaction media. It was particularly worth mentioning that **Azo-MOP-1** was obtained in 95% yield at 25 °C within 1 h by adopting acetonitrile as the solvent. Subsequently, using acetonitrile as the reaction medium, *t*-BuOCl/NaI as the organic oxidant, the oxidative polymerization of **A-N** (N=2~4) led to other three azo-containing networks, **Azo-MOP-N** (N=2~4), respectively, under quite mild conditions. Different from the azo-bridged MOPs prepared through direct coupling of nitro aromatic compounds and aromatic amines,[10a] the Azo-MOPs synthesized in this work had the sole chemical structural unit with terminal amino groups, which may have unique features. As known, the azo-type ligand is one of the most versatile ligands studied in coordination chemistry.[12] Herein, with azo-functional groups embedded in the skeletons, ruthenium-functionalized Azo-MOPs (**Azo-MOP-N-Ru,** N=1~4) was synthesized through the coordination of $RuCl_3 \cdot 3H_2O$ with the as-prepared Azo-MOPs via simply mixing.

The formation of **Azo-MOP-N** (N=1~4) was revealed by Fourier transform infrared (FTIR) spectroscopy, and cross-polarization magic-angle spinning (CP/MAS) ^{13}C NMR. In the FTIR spectra (Figure S3, ESI), the structures of -N=N- functionality were confirmed by the characteristic bands at 1147 and 1403 cm^{-1} due to the symmetric and asymmetric vibrations of the azo group,[10a] along with the respective bands for C-N stretching vibration (1280 cm^{-1}) and aromatic rings

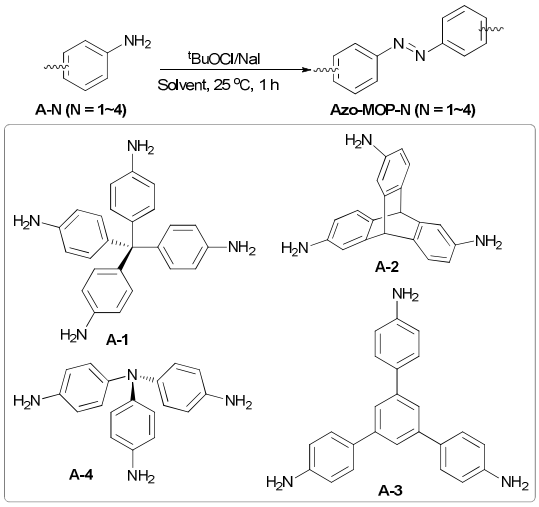

Scheme 1 Synthetic routes to the azo-containing networks **Azo-MOP-N** (N = 1~4).

(1450, 1500, 1580 and 1600 cm^{-1}). The FTIR bands located at 3437 and 3200 cm^{-1} corresponded to N-H stretching mode, suggesting the presence of unreacted terminal amino groups.[13] After coordinating with $RuCl_3 \cdot 3H_2O$, the stretching vibration for Ru-Cl bond (1076 cm^{-1}) and bending vibration for the bound H_2O molecule in $RuCl_3 \cdot 3H_2O$ (1609 cm^{-1}), was observed in the FTIR spectra of the obtained **Azo-MOP-N-Ru** (N=1~4) (Figure S4, ESI). The presence of chemical shifts in CP/MAS ^{13}C NMR spectra (Figure S5, ESI) of **Azo-MOP-N** (N = 1~4) located in the range of 113.3~152.1 ppm belonged to the aromatic carbons in the backbone, thus confirming the formation of the azo-linked aromatic polymers.[14] The quaternary carbon in **Azo-MOP-1** was located at 64.2 ppm, and the tertiary carbon in **Azo-MOP-2** was at 53.9 ppm.

For the as-prepared **Azo-MOP-N** (N=1~4), each sample cannot be dissolved in any solvents, implying the hypercrosslinked structure. The thermogravimetric analysis (TGA) of **Azo-MOP-N** (N=1~4) (Figure S6, ESI) indicated that they could be stable up to 400 °C in air. The mass losses could be assigned to desorption of trapped solvent molecules and the decomposition of the framework. The morphologies of **Azo-MOP-N** (N=1~4) and **Azo-MOP-N-Ru** (N=1~4) were observed by field-emission scanning electron microscopy (SEM) and transmission electron microscopy (TEM) (Figure S7, ESI). The **Azo-MOP-N** (N=1~4) samples were composed of tiny particles with irregular shape and size, and kept the morphology unchanged after coordinating with Ru complex. In addition, TEM images supported a very homogeneous ruthenium loading without detectable ruthenium clusters or nanoparticles in the **Azo-MOP-N-Ru** materials. The Ru content in each sample was almost identical, as determined by inductively coupled plasma-optical emission spectroscopy (ICP-OES) analysis, which were 4.67, 4.82, 4.70 and 4.65 wt% for **Azo-MOP-N-Ru** (N=1~4), respectively. X-ray photoelectron spectroscopy (XPS) measurements were performed to further investigate the oxidation state of

Journal Name View Article Online DOI: 10.1039/C5CC05151F ARTICLE

ruthenium, for example, in **Azo-MOP-3-Ru** (Figure S8, ESI). The four peaks with binding energies (BEs) of 281.42 eV ($Ru3d_{5/2}$), 285.12 eV ($Ru3d_{3/2}$, overlapping with the peak for C1s), 462.67 eV ($Ru3p_{3/2}$) and 484.67 eV ($Ru3p_{1/2}$) were consistent with those of the Ru species in the +3 state,[9] however, shifting to lower values compared to those of $RuCl_3$, suggesting the coordination of Ru(III) with azo functionality.

N_2 physisorption measurements at 77 K were performed in order to evaluate the pore structure of the **Azo-MOP-N** (N=1~4) (Figure S9, ESI). The isotherms displayed rapid sorption of N_2 at low relative pressure (< 0.01), indicative of the characteristics of permanent micropores (type I). The hysteresis at low pressures may be attributed to the pore networks effect[15] and also to the irreversible binding of gas molecules to the micropore surface. The Brunauer-Emmett-Teller (BET) surface areas of the resultant samples were found to be comparable to those of the reported azo-containing porous polymers,[10a] and increased in the order: **Azo-MOP-4** < **Azo-MOP-1** < **Azo-MOP-3** < **Azo-MOP-2** (Table 1, Figure S10, ESI). After coordination with $RuCl_3{\cdot}3H_2O$, both the BET surface area and the total pore volume were decreased from 335~706 m^2g^{-1} and 0.28~0.63 cm^3g^{-1} for **Azo-MOP-N** (N=1~4) to 61~370 m^2g^{-1} and 0.18~0.48 cm^3g^{-1} for **Azo-MOP-N-Ru** (N=1~4) (Figure S9 and Table 1). This was probably due to weight increase and tiny block of the cavities by Ru species (for pore size distribution, see Figure S11, ESI). The CO_2 uptakes of **Azo-MOP-N** (N=1~4) were investigated up to 1 bar at 273 K, and the results are illustrated in Figure S9 and Table 1. It is clear that the CO_2 isotherms were completely reversible, and **Azo-MOP-3** showed the highest adsorption capacity of 134.8 mg g^{-1} at 273 K. **Azo-MOP-1** with terminal amino groups had the same chemical structural unit as the reported **Azo-COP-1** obtained via the direct coupling of tetrakis(4-nitrophenyl)methane and tetrakis(4-aminophenyl)methane at 150 °C.[10a] However, **Azo-MOP-1** (456 m^2 g^{-1}) showed slightly lower BET surface area than **Azo-COP-1** (608 m^2 g^{-1}), which might be ascribed to the lower molecular weight of **Azo-MOP-1** because it was synthesized at room temperature. Interestingly, **Azo-MOP-1** (0.21 mg m^{-2}) had higher CO_2 capacity per unit surface area over **Azo-COP-1** (0.18 mg m^{-2}), which may be attributed to the presence of more amino groups in **Azo-MOP-1**. Especially, **Azo-MOP-4** with additional tertiary amine-functionality embedded in the backbone performed even better for CO_2 adsorption per unit surface area (0.23 mg m^{-2}). As expected, **Azo-MOP-2** with the highest BET surface area afforded the best CO_2 adsorption capacity (134.8 mg g^{-1}, S_{BET}: 706 m^2 g^{-1}). This value was even much higher than those of porous polymers with very high surface areas,[1] such as **CMP-1-(OH)** (79.2 mg g^{-1}, S_{BET}: 1043 m^2 g^{-1})[16] and **CMP-0** (92.4 mg g^{-1}, S_{BET}: 1018 m^2 g^{-1})[17]. The high affinity to CO_2 of **Azo-MOP-N** (N=1~4) may be a consequence of the favourable interactions of the polarizable CO_2 molecules through dipole-quadrupole interactions with the framework (azo functionality), terminal amino groups and also the inherent microporosity of **Azo-MOP-N** (N=1~4). The Ru-incorporated polymers also had the ability for CO_2 adsorption, as shown in Figure S9 and Table 1. However, the integration of Ru^{3+} decreased the adsorption capacity of CO_2, for instance, down to 92.1 mg g^{-1} from 134.8 mg g^{-1} for **Azo-MOP-2-Ru**, which might be caused by the decreased BET surface areas of the resultant materials and the coordination of CO_2-philic azo moieties with Ru species.

Table 1 Porosity parameters and CO_2 uptakes of the azo-containing networks **Azo-MOP-N** and **Azo-MOP-N-Ru** (N=1~4)

Samples	S_{BET} (m^2 g^{-1})	V_{total} (cm^3 g^{-1})	CO_2 uptake (mg g^{-1})	CO_2 uptake (mg m^{-2})
Azo-MOP-1	456	0.48	97.4	0.21
Azo-MOP-2	706	0.53	134.8	0.19
Azo-MOP-3	523	0.63	81.2	0.16
Azo-MOP-4	335	0.28	77.7	0.23
Azo-COP-1[a]	608	0.39	107.6	0.18
Azo-MOP-1-Ru	154	0.27	59.5	0.39
Azo-MOP-2-Ru	326	0.28	92.1	0.28
Azo-MOP-3-Ru	370	0.48	82.1	0.22
Azo-MOP-4-Ru	61	0.18	52.8	0.87

a The result obtained from Ref. [10].

From the above results, it is clear that the resultant Azo-MOPs are good sorbents for CO_2 capture, and they are expected to have good performance for CO_2 conversion. The methylation of amines using CO_2 as a C1 resource is a green route, which has been investigated recently. The product methylamines are basic reagents in nitrogen chemistry, which are generally used as platform chemicals or solvents, etc. However, in most cases complicated catalysts and harsh conditions (e.g., high temperature and pressure) were required.[18] The heterogeneous catalyst for the methylation of amines under mild conditions is seldom reported. In this work, the resultant **Azo-MOP-N-Ru** (N=1~4) were applied in the methylation of amines using CO_2 as a C1 building block. As shown in Table 2, the reaction of N-methylaniline (**1a**) and CO_2 in the presence of $PhSiH_3$ proceeded well catalyzed by **Azo-MOP-N-Ru** (N=1~4), producing N,N-dimethylaniline (**2a**) in 89~99% yields under low CO_2 pressure (0.5 MPa) within 24 h (entries 1-4). Among the tested **Azo-MOP-N-Ru** (N=1~4), **Azo-MOP-3-Ru** displayed the superior catalytic activity. The difference in the catalytic activities of **Azo-MOP-N-Ru** (N=1~4) was probably due to their discriminatory BET surface areas and pore size distributions. In comparison, the resultant **Azo-MOP-N-Ru** (N=1~4) showed better performances than the reported homogeneous catalytic system $[RuCl_2(dmso)_4]$/$nBuPAd_2$ that required a high CO_2 pressure (e.g., 3 MPa) to afford **2a** in a comparable yield of 92%.[19] In addition, it was demonstrated that the catalytic activity of **Azo-MOP-N-Ru** (N=1~4) was superior to that of homogeneous $RuCl_3{\cdot}3H_2O$ (entries 1-4 vs. 5), probably owing to the synergistic effects between the Azo-MOPs support and the Ru species. Most importantly, the catalyst **Azo-MOP-3-Ru** showed good reusability, confirmed by the fact that 95% yield of **2a** was obtained after the catalyst was reused for five times (Figure S12, ESI). The TEM images indicated that the Ru(III) species was still highly homogeneous after recycling five times (Figure S13, ESI). In addition, there was no Ru species detected in the filtrate of the reaction mixture, indicating the strong coordination ability of Ru(III)

View Article Online
DOI: 10.1039/C5CC03153F

species with the azo-type ligand and the excellent stability of **Azo-MOP-3-Ru** as an efficient heterogeneous catalyst.

Table 2 Azo-MOP-N-Ru-catalyzed methylation of N-methylaniline (**1a**) using CO_2 as a C1 building block[a]

Entry	Catalyst	**1a** Conv.(%)[b]	**2a** yield(%)[b]
1	**Azo-MOP-1-Ru**	98	92
2	**Azo-MOP-2-Ru**	98	94
3	**Azo-MOP-3-Ru**	100	99
4	**Azo-MOP-4-Ru**	98	89
5	$RuCl_3 \cdot 3H_2O$	74	64

[a] Reaction conditions: **1a** 0.5 mmol, catalyst loading 4 mol% Ru based on **1a**, PPh_3 0.1 mmol, organosilane $PhSiH_3$ 4 mmol, CO_2 pressure 0.5 MPa, solvent THF 2 mL, 120 ºC, 24 h. [b] Determined by GC using dodecane as an internal standard.

Azo-MOP-3-Ru could be applied to the reactions of various amines with CO_2 under low pressure (0.5 MPa) (Table S1, ESI). N-methylanilines with both electron-donating (Entries 2-5) and electron-withdrawing groups (Entries 6-10) could be transformed to the corresponding N,N-dimethylanilines in excellent yields (93-99%). In addition, N-methylanilines with substituted groups (Cl- or CH_3-) on the ortho, meta- and para-positions of the benzene ring all converted to methylamines in excellent yields (Entries 2-4, 8-10). Dialkylamines also showed good reactivity (92% yield) catalyzed by **Azo-MOP-3-Ru** (Entry 11). The reduction of formamide was carried out, forming N,N-dimethylaniline (**2a**) solely in 99% yield catalyzed by **Azo-MOP-3-Ru** under the same other conditions (Entry 12), thus indicating the presence of the formamides intermediate during the reaction process.

To further gain insight into the facilitation of azo-functionalized materials to the methylation reaction of amines, NMR technique was employed to identify the interaction of **1a** and azo functionality, by taking an azo-containing monomer (azobenzen) instead of the insoluble Azo-MOPs (Figure S14, ESI). It was found that the proton signal of N-H bond in **1a** (H-2) showed a slightly upfield shift from 2.76 to 2.80 ppm after the addition of azobenzene, probably owing to the formation of hydrogen bond between N-H and electron-giving azo group. Correspondingly, inductive effect caused decrease in the electron density on the N atom of **1a**, thus leading to downfield shift of the other protons in the methyl group (H-1) and the benzene ring (H-3 to H-5), which was further proved by the downfield shift of the N signal in **1a** from 51.32 to 52.75 ppm. On the basis of the experimental results obtained, it can be deduced that the Azo-MOPs developed herein served as functionalized materials for efficient CO_2 adsorption/activation, showed strong coordinating ability with Ru species, activated N-H containing amines through hydrogen bond formation and thus displayed high efficiency for the methylation reaction of amines using CO_2 as a C1 building block. A possible mechanism for the methylation of amines with captured CO_2 by Azo-MOP-3-Ru was proposed as shown in Scheme S1 (ESI).

In summary, we have elaborated a novel, simple and efficient method for the synthesis of azo-functionalized MOPs in excellent yields (> 95%) at room temperature. The resultant Azo-MOPs with BET surface areas up to 706 $m^2\ g^{-1}$ displayed high thermal stability and high adsorption capacity to CO_2. In addition, the azo-type ligands within the skeletons showed excellent coordinating ability for Ru-complex. Efficient methylation of amines using CO_2 as C1 building block was realized adopting the resultant Azo-MOP-Ru as catalyst, thus providing a new direction for the simultaneous adsorption, activation and transformation of CO_2 into value-added chemicals under mild conditions.

The authors thank the National Natural Science Foundation of China (No. 21125314, 21321063, 21402208) for the financial support.

Notes and references

1 Y. Xu, S. Jin, H. Xu, A. Nagai and D. Jiang, *Chem. Soc. Rev.*, 2013, **42**, 8012-8031.
2 D. Wu, F. Xu, B. Sun, R. Fu, H. He and K. Matyjaszewski, *Chem. Rev.*, 2012, **112**, 3959-4015.
3 A. Thomas, *Angew. Chem. Int. Ed.*, 2010, **49**, 8328-8344.
4 N. Du, H. B. Park, G. P. Robertson, M. M. Dal-Cin, T. Visser, L. Scoles and M. D. Guiver, *Nat. Mater.*, 2011, **10**, 372-375.
5 M. G. Rabbani and H. M. El-Kaderi, *Chem. Mater.*, 2011, **23**, 1650-1653.
6 R. Dawson, E. Stockel, J. R. Holst, D. J. Adams and A. I. Cooper, *Energy Environ. Sci.*, 2011, **4**, 4239-4245.
7 Y. Zhang and S. N. Riduan, *Chem. Soc. Rev.*, 2012, **41**, 2083-2094.
8 Y. Xie, T.-T. Wang, X.-H. Liu, K. Zou and W.-Q. Deng, *Nat. Commun.*, 2013, **4**, 1960-1967.
9 Z.-Z. Yang, H. Zhang, B. Yu, Y. Zhao, G. Ji and Z. Liu, *Chem. Commun.*, 2015, **51**, 1271-1274.
10 (a) H. A. Patel, S. Hyun Je, J. Park, D. P. Chen, Y. Jung, C. T. Yavuz and A. Coskun, *Nat. Commun.*, 2013, **4**, 1357; (b) P. Arab, M. G. Rabbani, A. K. Sekizkardes, T. İslamoğlu and H. M. El-Kaderi, *Chem. Mater.*, 2014, **26**, 1385-1392; (c) J. Lu and J. Zhang, *J. Mater. Chem. A*, 2014, **2**, 13831-13834; (d) H. A. Patel, S. H. Je, J. Park, Y. Jung, A. Coskun and C. T. Yavuz, *Chem. Eur. J.*, 2014, **20**, 772-780.
11 (a) K. Muñiz and M. Nieger, *Angew. Chem. Int. Ed.*, 2006, **45**, 2305-2308; (b) D. Garn, F. Knoch and H. Kisch, *J. Organomet. Chem.*, 1993, **444**, 155-164; (c) A. K. Mahapatra, S. Datta, S. Goswami, M. Mukherjee, A. K. Mukherjee and A. Chakravorty, *Inorg. Chem.*, 1986, **25**, 1715-1721.
12 A. L. Balch and D. Petridis, *Inorg. Chem.*, 1969, **8**, 2247-2252.
13 L. M. Sáiz, P. A. Oyanguren and M. J. Galante, *React. Funct. Polym.*, 2012, **72**, 478-485.
14 T. Ben, H. Ren, S. Ma, D. Cao, J. Lan, X. Jing, W. Wang, J. Xu, F. Deng, J. M. Simmons, S. Qiu and G. Zhu, *Angew. Chem. Int. Ed.*, 2009, **48**, 9457-9460.
15 N. B. McKeown and P. M. Budd, *Chem. Soc. Rev.*, 2006, **35**, 675-683.
16 R. Dawson, D. J. Adams and A. I. Cooper, *Chem. Sci.*, 2011, **2**, 1173-1177.
17 S. Ren, R. Dawson, A. Laybourn, J.-x. Jiang, Y. Khimyak, D. J. Adams and A. I. Cooper, *Polym. Chem.*, 2012, **3**, 928-934.
18 A. Tlili, X. Frogneux, E. Blondiaux and T. Cantat, *Angew. Chem. Int. Ed.*, 2014, **53**, 2543-2545.
19 Y. Li, X. Fang, K. Junge and M. Beller, *Angew. Chem. Int. Ed.*, 2013, **52**, 9568-9571.